

Catalytic evaluation of MOF-808 with metallic centers of Zr(IV), Hf (IV) and Ce(IV) in the acetalization of benzaldehyde with methanol

Yazmín Arellano^{a,b}, César Pazo^{a,b}, Vanesa Roa^{a,b}, Yoan Hidalgo-Rosa^c, Ximena Zarate^d,

Jaime Llanos^e, Nestor Escalona^{b,f,g} and Eduardo Schott^{a,b*}

^a Departamento de Química Inorgánica, Facultad de Química y de Farmacia, Centro de Energía UC, CIEN-UC, Pontificia Universidad Católica de Chile, Avenida Vicuña Mackenna, 4860, Santiago, Chile.

^b ANID-Millennium Science Initiative Program-Millennium Nuclei on Catalytic Process Towards Sustainable Chemistry (CSC), Chile.

^c Centro de Nanotecnología Aplicada, Facultad de Ciencias, Ingeniería y Tecnología, Universidad Mayor, Camino La Pirámide 5750, Huechuraba, Santiago, Chile, 8580745.

^d Instituto de Ciencias Aplicadas, Facultad de Ingeniería, Universidad Autónoma de Chile, Santiago, Chile.

^e Departamento de Química, Facultad de Ciencias, Universidad Católica del Norte, Antofagasta, Chile.

^f Departamento de Ingeniería Química y Bioprocessos, Escuela de Ingeniería, Pontificia Universidad Católica de Chile, Avenida Vicuña Mackenna 4860, Macul, Santiago, Chile.

^g Departamento de Química Física, Facultad de Química y de Farmacia, Pontificia Universidad Católica de Chile, Vicuña Mackenna 4860, Santiago, Chile.

*maschotte@gmail.com

Table of contents

1.Characterization of MOF-808-M	3
---------------------------------------	---

2. Computational study.....	9
2.1 Cluster models (finite fragments of MOF-808-M).....	9
2.2 Molecular geometry results	11
3. Reference	14

1. Characterization of MOF-808-M

Table S1. Potentiometric acidity for MOF-808-Zr, MOF-808-Hf y MOF-808-Ce studied.

	pKa1	pKa2	pKa3
MOF	$\mu_3\text{-OH}$	M-OH_2	M-OH
MOF-808-Zr	3.65	5.93	8.08
MOF-808-Hf	3.26	5.68	7.85
MOF-808-Ce	3.23	6.35	7.97

Table S2. Molecular formula, molecular mass and defects calculated for MOF-808-Zr, MOF-808-Hf y MOF-808-Ce by potentiometric titration.

MOF	Molecular formula	Molecular mass (g/mol)	Defects
MOF-808-Zr	$\text{Zr}_6\text{O}_4(\mu_3\text{-OH})_4(\text{OH})_6(\text{H}_2\text{O})_6(\text{C}_9\text{H}_3\text{O}_6)_{1.56}[(\text{H}_2\text{O})(\text{OH})]_{1.32}$	1258.83	0.39
MOF-808-Hf	$\text{Hf}_6\text{O}_4(\mu_3\text{-OH})_4(\text{OH})_6(\text{H}_2\text{O})_6(\text{C}_9\text{H}_3\text{O}_6)_{1.61}[(\text{H}_2\text{O})(\text{OH})]_{1.17}$	1788.55	0.39
MOF-808-Ce	$\text{Ce}_6\text{O}_4(\mu_3\text{-OH})_4(\text{OH})_6(\text{H}_2\text{O})_6(\text{C}_9\text{H}_3\text{O}_6)_{1.13}[(\text{H}_2\text{O})(\text{OH})]_{2.61}$	1508.33	0.87

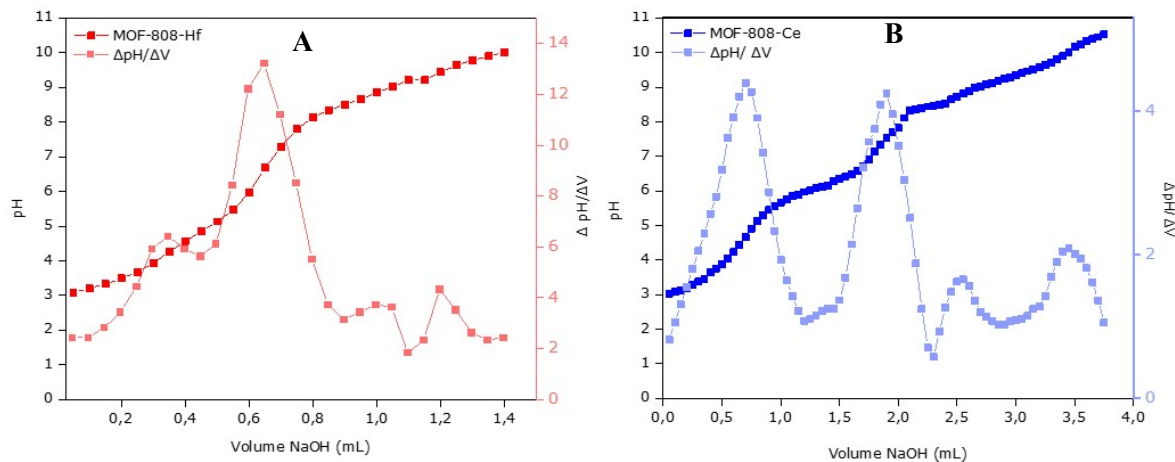


Figure S1. Acid- base potentiometric titration and its first derivative curve of MOF-808-Hf (**A**) and MOF-808-Ce (**B**).

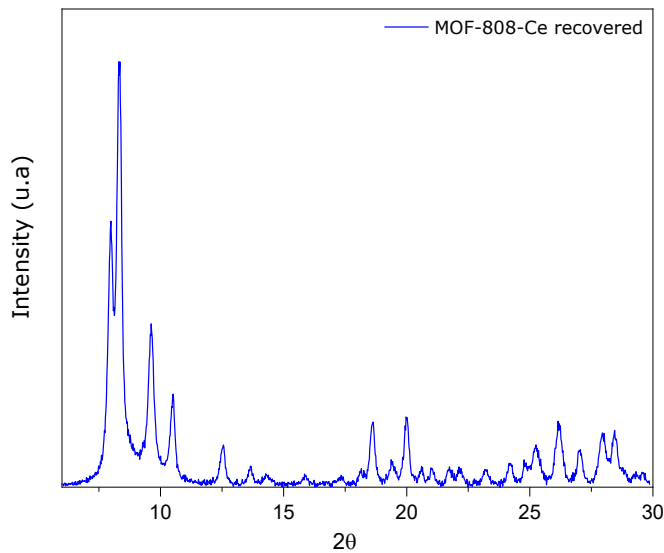


Figure S2. Diffraction pattern MOF-808-Ce recovered.

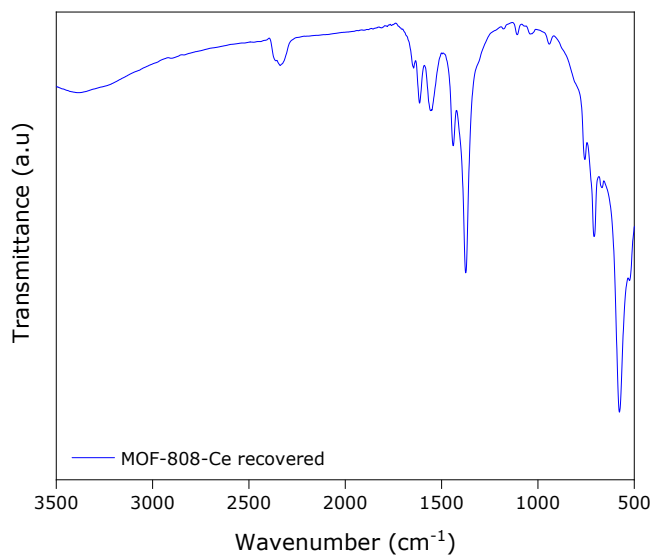


Figure S3. ATR-FTIR spectra MOF-808-Ce recovered.

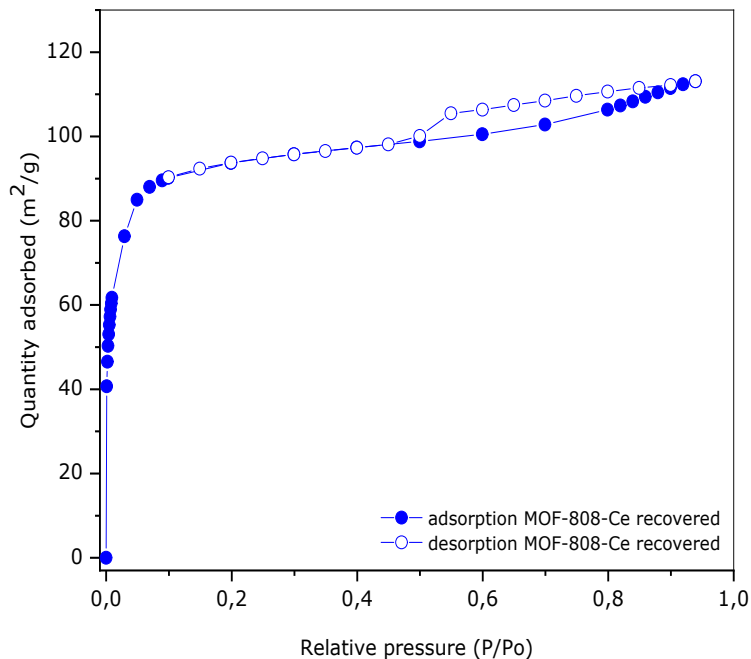


Figure S4. N_2 adsorption and desorption isotherm of recovered MOF-808-Ce.

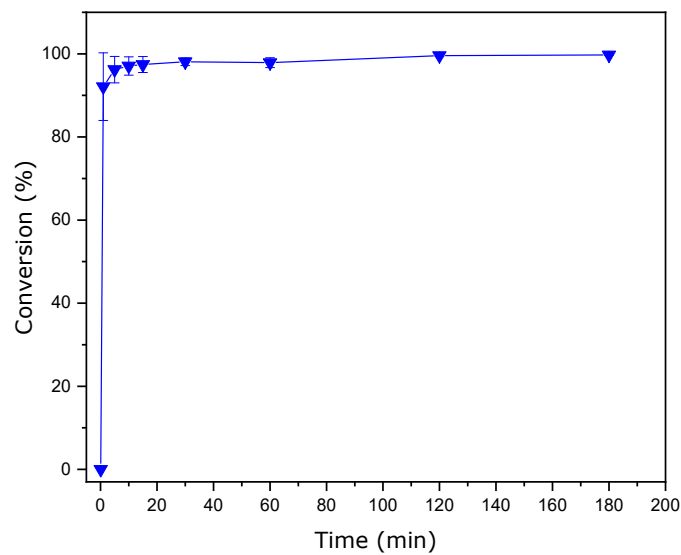


Figure S5. Conversion versus time in the acetalization of benzaldehyde with methanol catalyzed by MOF-808-Ce in the initial conditions (330 μL of benzaldehyde and 10 mL).

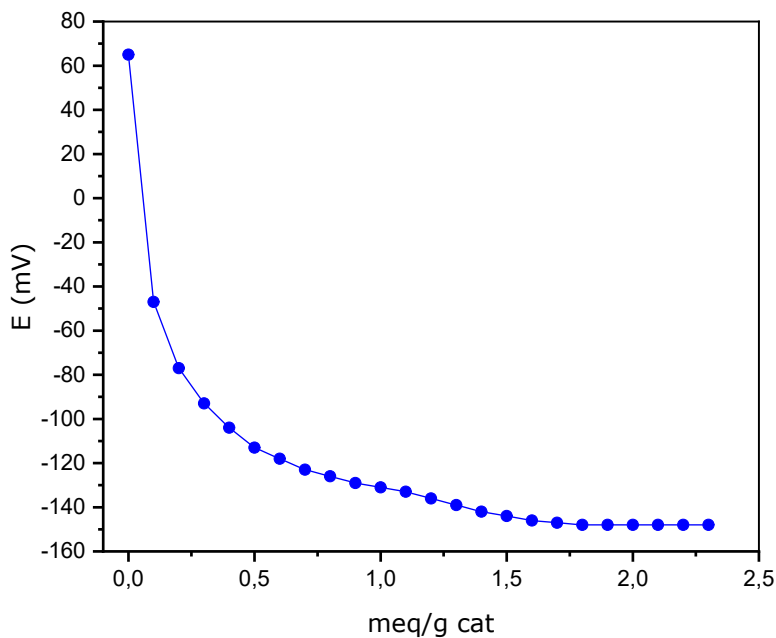


Figure S6. Potentiometric titration curve with butylamine in acetonitrile of MOF-808-Ce recovered post catalytic cycle.

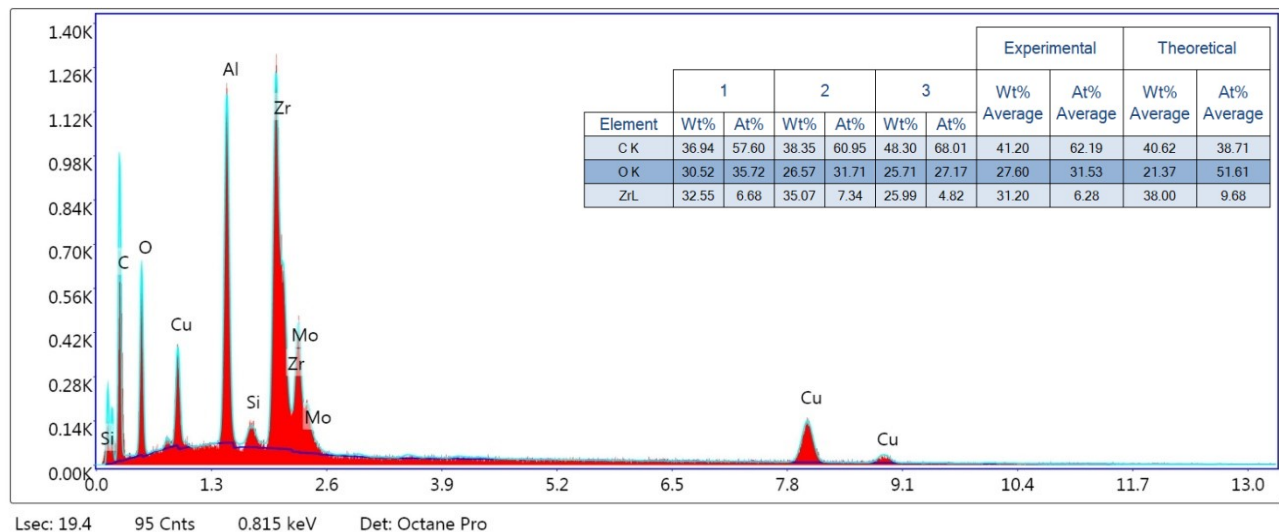


Figure S7. EDS MOF-808-Zr.

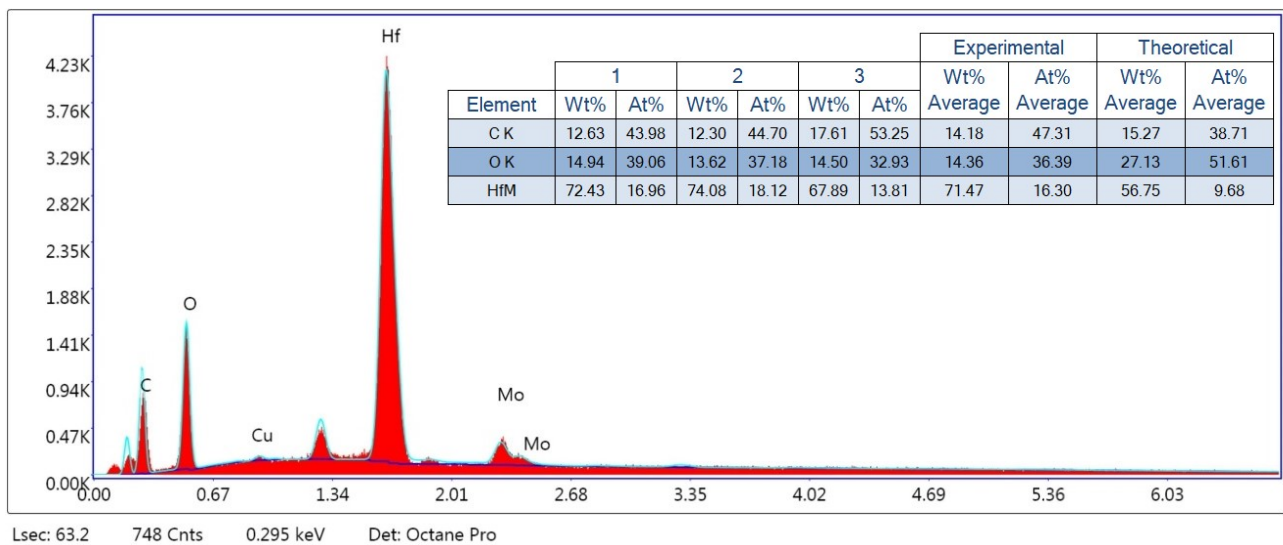


Figure S8. EDS MOF-808-Hf.

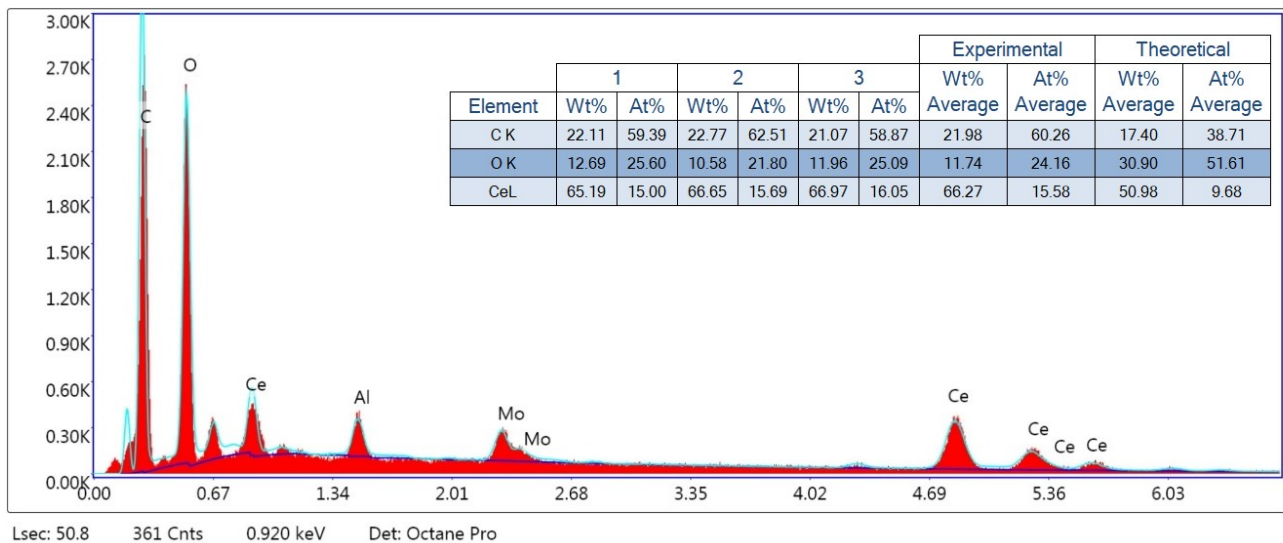


Figure S9. EDS MOF-808-Ce.

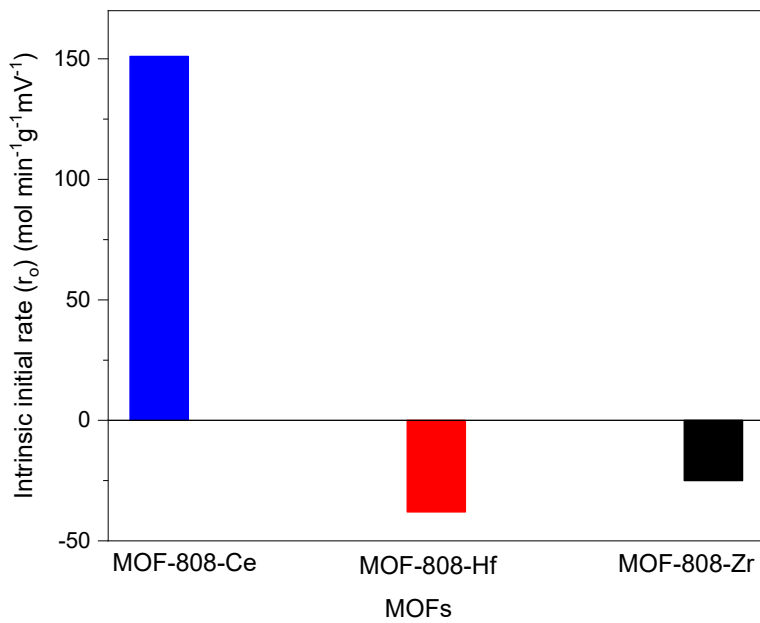


Figure S10. Normalization of the initial rate using strong acid of different materials.

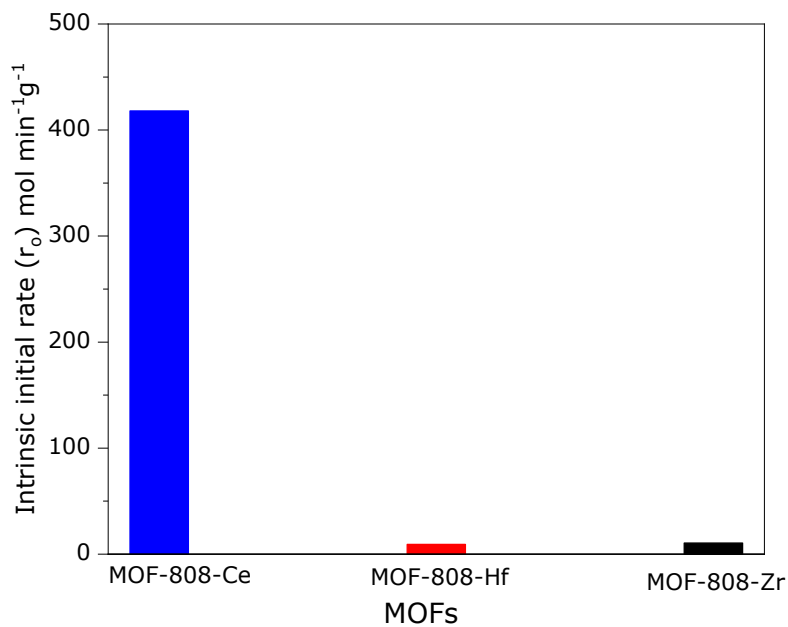


Figure S11. Normalization of initial rate by number of defects in materials.

2. Computational study

2.1 Cluster models (finite fragments of MOF-808-M)

The theoretical study of MOFs can be complex due to of their large size, making computational simulations challenging due to high computational costs [3]. To address this, a strategy of truncating the periodic structure into a smaller representative fragment, named cluster model, has been developed. This method involves selecting a fragment from the MOF that correctly embodies the overall structure, maintaining its properties of interest [1]. This smaller fragment allows for detailed computational analysis that would otherwise not be possible with the full MOF structure [2].

The use of truncated cluster models is particularly useful for studying phenomena such as catalysis, chemical detection, and gas separation, which occur or have properties arising from highly localized electronic states [4]. However, the process of truncation is not without difficulties. It's crucial to ensure the chosen fragment is representative of the extended systems. Thus, necessitating an in-depth understanding of the MOF's structure and properties and careful consideration of truncation's potential impact on simulation results.

In this work for MOF-808-M a representative fragment is based on the secondary building unit (SBU), which consists of the fragments $[M_6O_4(OH)_4(H_3BTC)_5(HCOO)_6]^{+1}$, ($M = Ce^{4+}, Zr^{4+}$, and Hf^{4+}). In these cluster models was considered one defect site arising from missing linkers, see Figure 12. The crystal structure for MOF-808-Zr [5] was used as template to create the cluster model of each material (we will referred as MOF-808-Zr, MOF-808-Hf and MOF-808-Ce). From a theoretical standpoint was exploring intermolecular interactions of benzaldehyde and methanol with the MOF-808-M.

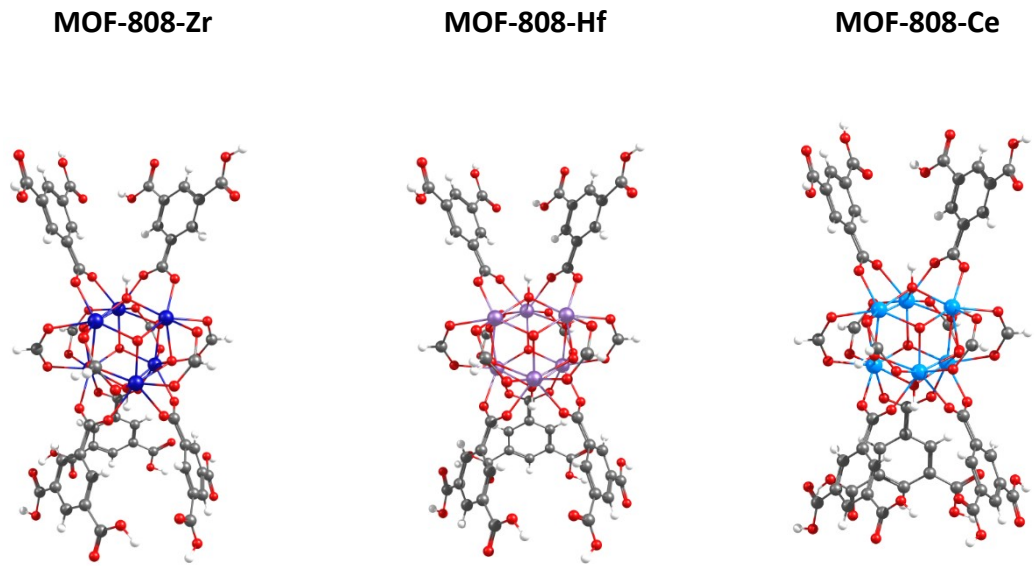


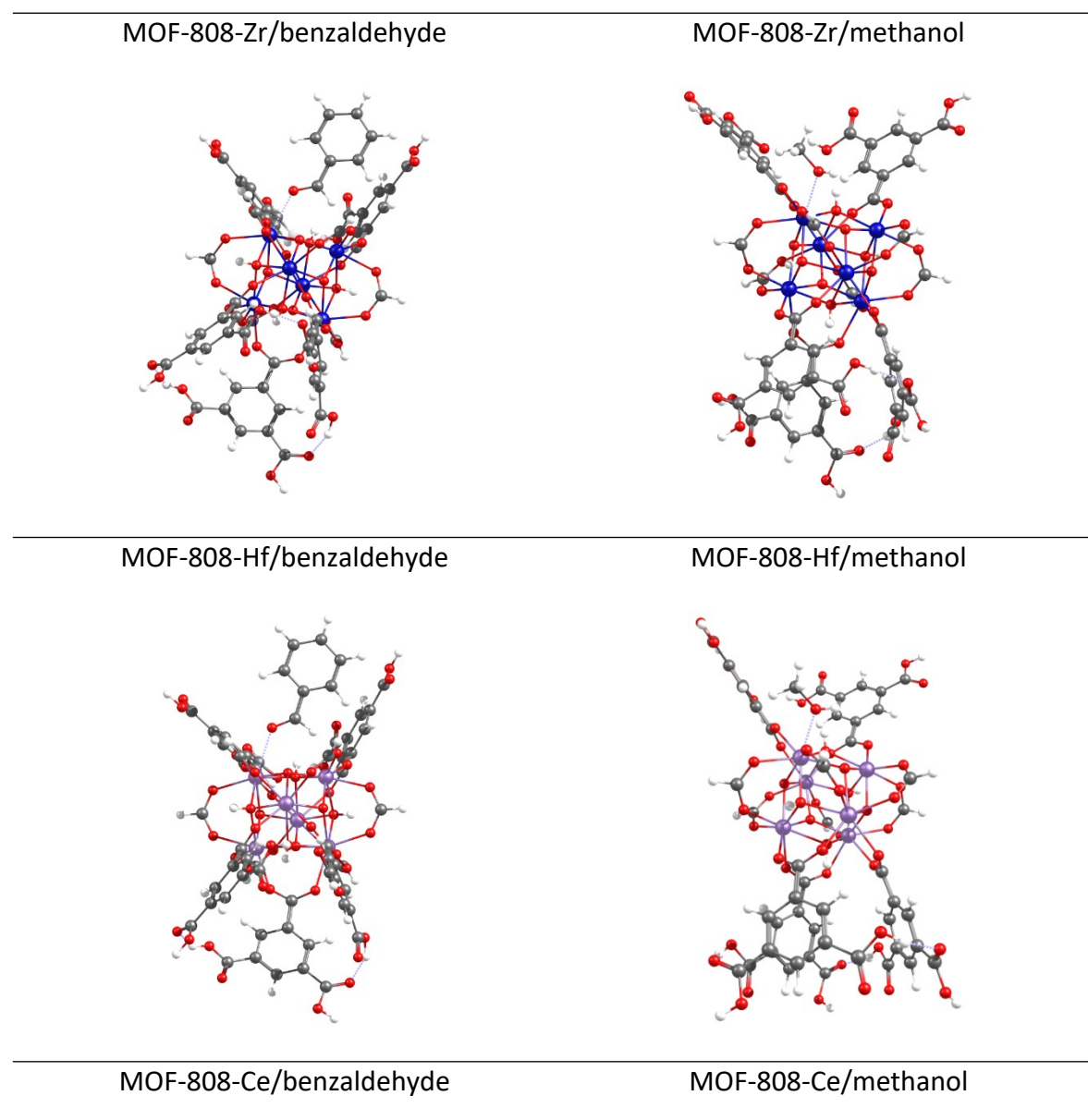
Figure S12. Optimized geometry of the $[\text{Me}_6\text{O}_4(\text{OH})_4(\text{H}_3\text{BTC})_5(\text{HCOO})_6]^{+1}$ structural model ($\text{M} = \text{Ce}^{4+}$, Zr^{4+} , and Hf^{4+}).

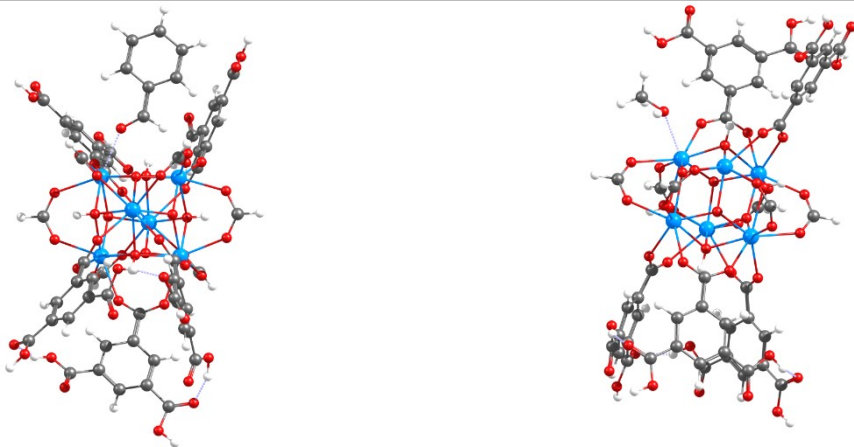
2.2 Molecular geometry results

The results of the geometry optimization on the cluster model MOF-808-Zr MOF align well with the experimental data reported by Omar M. Yaghi for the extended systems [5]. The data revealed that the calculated bond lengths of $[Zr-O(\mu_3-OH), Zr-O(\mu_3-O), Zr-O(COOH) \text{ and } Zr-O(H_3BTC)]$ are 2.22, 2.06, 2.21 and 2.22 Å respectively. In comparison, the experimental data for MOF-808-Zr [5] are 2.22, 2.06, 2.26 and 2.21 Å respectively. Based on this result all MOF-808-M/benzaldehyde and MOF-808-M/methanol systems were optimized at the same theoretical level as the free MOF-808-M.

Table S3 in the Supporting Information display optimized geometries of the MOF-808-M/benzaldehyde and MOF-808-M/methanol systems at the ground state (S_0) electronic state. In all four systems, it is possible to observe that the host-guest interaction converged to the guest (benzaldehyde or methanol) interacting with in the defect sites on node of MOF-808-M (host). For all host-guest systems final conformations show that the benzaldehyde carbonyl and methanol hydroxyl group are oriented towards to defect sites (such as the Lewis (M: Ce, Hf or Zr) and Brønsted (μ_3-OH and μ_3-O) sites) closer to the metal site.

Table S3. Optimized structure of all simulated interacting system in the ground state at BP86/TZ2P





Color coding: red = oxygen, gray = carbon, white = hydrogen, blue = Zirconium, Light Blue
= Cerium and Purple =Hafnium.

3. Reference

- [1] Hidalgo-Rosa, Y., Treto-Suárez, M. A., Schott, E., Zarate, X., & Páez-Hernández, D. (2020). Sensing mechanism elucidation of a europium(III) metal–organic framework selective to aniline: A theoretical insight by means of multiconfigurational calculations. *Journal of Computational Chemistry*, 41(22), 1956–1964. <https://doi.org/10.1002/JCC.26365>
- [2] Mancuso, J. L., Mroz, A. M., Le, K. N., & Hendon, C. H. (2020). Electronic Structure Modeling of Metal-Organic Frameworks. *Chemical Reviews*, 120(16), 8641–8715. <https://doi.org/10.1021/acs.chemrev.0c00148>
- [3] McCarver, G. A., Rajeshkumar, T., & Vogiatzis, K. D. (2021). Computational catalysis for metal-organic frameworks: An overview. *Coordination Chemistry Reviews*, 436, 1–73. <https://doi.org/10.1016/j.ccr.2021.213777>
- [4] Odoh, S. O., Cramer, C. J., Truhlar, D. G., & Gagliardi, L. (2015). Quantum-Chemical Characterization of the Properties and Reactivities of Metal-Organic Frameworks. In *Chemical Reviews* (Vol. 115, Number 12, pp. 6051–6111). <https://doi.org/10.1021/cr500551h>
- [5] Trickett, C. A., Osborn Popp, T. M., Su, J., Yan, C., Weisberg, J., Huq, A., Urban, P., Jiang, J., Kalmutzki, M. J., Liu, Q., Baek, J., Head-Gordon, M. P., Somorjai, G. A., Reimer, J. A., & Yaghi, O. M. (2019). Identification of the strong Brønsted acid site in a metal–organic framework solid acid catalyst. *Nature Chemistry*, 11(2), 170–176. <https://doi.org/10.1038/s41557-018-0171-z>